A Multi-wavelength IR Laser for space applications

Steven X. Li, Anthony W. Yu, Xiaoli Sun, Molly E. Fahey, Kenji Numata and Michael A. Krainak
NASA Goddard Space Flight Center, 8800 Greenbelt Road, Greenbelt, MD 20771

ABSTRACT

We present a laser technology development with space flight heritage to generate laser wavelengths in the near- to mid-infrared (NIR to MIR) for space lidar applications. Integrating an optical parametric crystal to the LOLA (Lunar Orbiter Laser Altimeter) laser transmitter design affords selective laser wavelengths from NIR to MIR that are not easily obtainable from traditional diode pumped solid-state lasers. By replacing the output coupler of the LOLA laser with a properly designed parametric crystal, we successfully demonstrated a monolithic intra-cavity optical parametric oscillator (iOPO) laser based on all high technology readiness level (TRL) subsystems and components. Several desired wavelengths have been generated including 2.1 µm, 2.7 µm and 3.4 µm. This laser can also be used in trace-gas remote sensing, as many molecules possess their unique vibrational transitions in NIR to MIR wavelength region, as well as in time-of-flight mass spectrometer where desorption of samples using MIR laser wavelengths have been successfully demonstrated.

Keywords: Optical parametric oscillator, iOPO, laser, lidar, infrared.

1. INTRODUCTION

The Moon polar environment experiences permanent shadow where temperatures are extremely low. This enables cold-trapping of volatiles and allows retention of water ice [1, 2]. Reflectance measurements at a few wavelengths near 3 µm and supporting reference wavelengths can definitively answer the question of whether water detected by passive spectrometers is mobile by comparing day and night band depths which in turn constrains the supply of water to permanently shadowed regions at the poles. The 3-µm region is uniquely sensitive to the presence of all water bearing species and the instrument can measure the abundance of water ice in permanent shadow to the lunar background water abundance of less than 100 parts per million (ppm), far below the abundance accessible to shorter wavelength measurements.

For icy satellites, the lidar reflectance measurements near 3 µm can provide high quality characterization of dynamic processes at polar region independent of the sunlight. A NIR-MIR lidar can be used to map the fall-out of plumes from Enceladus and possibly Europa, and to characterize the properties of the plumes, such as the ratio of ice to non-icy species, organics and salts, and will provide invaluable support to the understanding of in situ measurements of plume materials, including life detection experiments.

Key to our understanding of Titan as a habitable moon is the relationship between its sub-surface water ocean, where energy is available from tidal dissipation, and its surface and atmosphere. Titan's surface is only visible in the VIS-NIR through a handful of narrow windows due to its atmospheric haze scatters light, particularly at shorter wavelengths. A laser altimeter may penetrate the atmosphere or even polar hood by choosing the laser wavelength at one of the transparent bands in the MIR. One promising window for surface measurement is centered at 2.03 µm with a 3 dB window between 1.99 to 2.08 µm.

A NIR to MIR laser reflectance measurement complement passive spectrometer measurements. Passive infrared spectral remote sensing can very accurately measure sunlight reflected off a planet's surface. These measurements can be compared to a reference spectrum to determine the mineral or chemical composition of a body. While passive spectral imaging is an exceedingly powerful technique, it is not without its shortcomings. The limitations imposed by the temperature of the source or the intensity of the sun, and the need to photometrically normalize the data can lead to artifacts or poorly unknown uncertainties. Active remote sensing can overcome these limitations.

The primary objective of this iOPO laser transmitter development is for a multi-wavelength infrared lidar instrument to detect and measure water ice on the Moon, comets and other airless bodies. By selecting proper nonlinear crystal cutting orientation, we can generate a wide range of wavelengths of interest.

1.1 Multi-wavelength Infrared Lidar instrument

Infrared laser spectroscopy is a powerful tool for the detection of the source and sink of important atmospheric gases and water related species. Numerous atmospheric gases including water vapor (H_2O), carbon dioxide (CO_2) and methane (CH_4) have very strong molecular-vibration absorption lines in the MIR, 2 to 5 µm range. LOLA and MLA [3, 4] provided quantitative reflectance data in regions of permanent shadow on the Moon. However, these single band laser reflectance measurements are insufficient to resolve volatile species.

At NASA Goddard Space Flight Center, we have been developing a new lidar instrument, similar to LOLA but with multiple infrared wavelengths, to measure the surface reflectance to ambiguously determine the abundance of volatiles on the moon. It extends the use of lidar from laser ranger to laser spectrometer. The laser wavelengths can be chosen to target specific compounds and minerals on the surface, as shown in Figure 1.

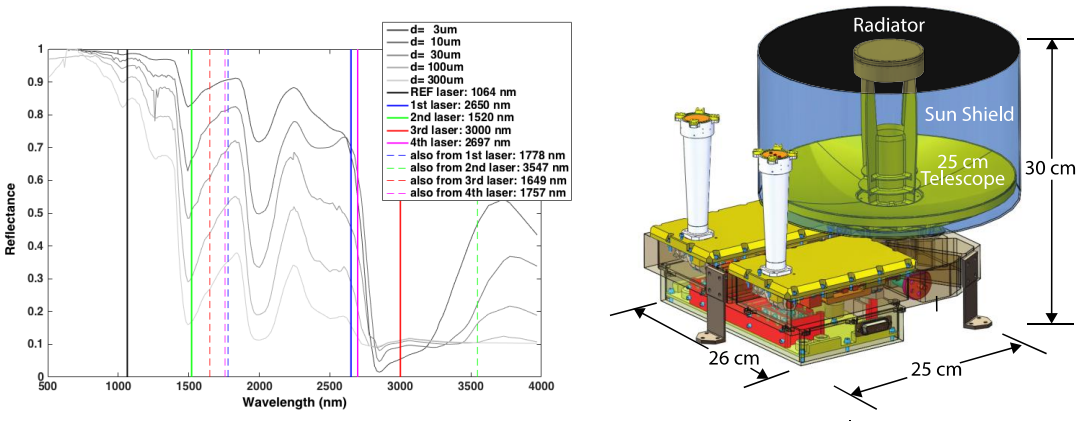

Figure 1. Radiative transfer models of spectral changes due to water and ice abundance, left. The multi-wavelength lidar measures the spectral absorption at the 3-µm laser wavelength, which has a strong absorption and unambiguous feature of water ice. Right shows the conceptual layout of multi-wavelength lidar instrument.

A highly reliable, compact, space qualifiable multi-wavelength MIR laser transmitter is key for this lidar instrument. The laser requirements for the multi-wavelength lidar are summarized in Table 1.

Laser transmitter parameter	
Laser Pulse Rate (Hz)	100
Laser pulse width (ns)	< 10
Transmitted pulse energy at 2.9 - 3.4 µm (µJ)	200
Transmitted pulse energy at 2.7 µm (µJ)	200
Transmitted pulse energy at 1.5-1.7 µm (µJ)	500
Transmitted pulse energy at 1.064 µm (µJ)	500

Table 1. Requirement for the multi-wavelength lidar laser transmitter.

2. INTRACAVITY OPTICAL PARAMETRIC OSCILATOR

The theory of intracavity optical parametric oscillator (iOPO) lasers has long been developed [5, 6]. They have not been widely used for spectroscopy measurements due to relatively wide spectral line-width (~1 nm) and difficulty of continuous wavelength tuning. However, iOPO lasers are well suited for the water ice measurement where the spectral absorption feature is broad and can be probed with a few discrete laser wavelengths. The iOPO takes advantage of the high fluence and longer pump duration inside the laser cavity, which greatly reduces the OPO threshold and increases the conversion efficiency. The primary interest in iOPO lasers for space applications is to reduce the cost, size and

weight. It enables us to use our LOLA and Mercury Laser Altimeter (MLA) heritages for iOPO laser design and development. Similar iOPO crystals have been used in other types of lasers that have flown in space. Figure 2 shows the iOPO laser operation principle schematic. The pump head is a laser gain medium, in our case, it is a diode pumped Nd:YAG crystal. M_1 is a high reflection (HR) mirror at pump wavelength, λ_p. M_2 is an iOPO middle mirror coated for high transmission (HT) at λ_p and HR at signal wavelength, λ_s. M_3 is an iOPO output coupler coated HR at λ_p, partial refection at signal wavelength λ_s and HT at idler wavelength λ_i. Mirrors M_1 and M_3 form a high finesse laser cavity that yields a very high intra-cavity intensity for pumping the nonlinear crystal. M_2, M_3 and a nonlinear crystal form a singly resonant optical parametric oscillator which generates signal wavelength λ_s and idler wavelength λ_i.

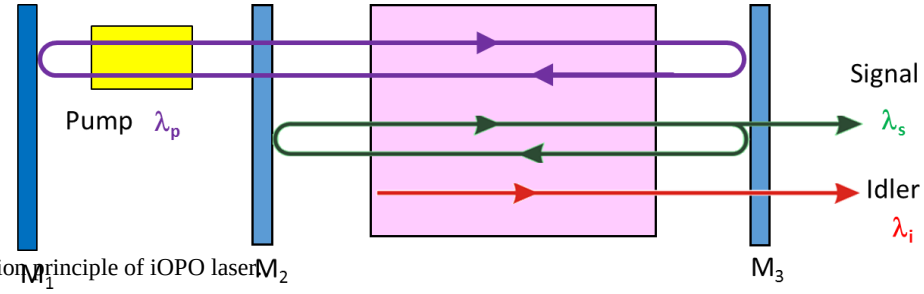

Figure 2. Operation principle of iOPO laser

We have developed a diode pumped monolithic intracavity optical parametric oscillator (iOPO) to generate required wavelengths for multi-wavelength lidar instrument [7, 8]. We modified our LOLA Engineering Model (EM) to demonstrate the required performance. The LOLA laser instrument consists of two identical diode-pumped, passively Q-switched Nd:YAG lasers [9]. We modified one of the two lasers into an iOPO by replacing the output coupler section with a monolithic iOPO crystal, as shown in Figures 3. The advantage of this iOPO laser design are the high wavelength conversion efficiency, and the heritage from the LOLA laser. The two LOLA lasers have been operating in space since 2009 [10] and have accumulated more than 4.2 billion laser shots each since launch in 2009 [11]. We can reuse essentially all flight qualified LOLA mechanical and optical design. The iOPO oscillator is composed of a Porro prism as a high reflector, a Brewster's angle cut Nd:YAG slab pumped by two two-bar stack (G2 package) of GaInAsP laser diode bars, a passive Q-switch (Cr^{4+}:YAG, 0.29 optical density), and Risley wedges used for optical alignment. A nonlinear crystal (KTA or KTP) cut for the desired phase matching angle is polished and coated for the desired operation wavelengths. The crystal end surfaces are parallel polished and coated to form a monolithic iOPO cavity.

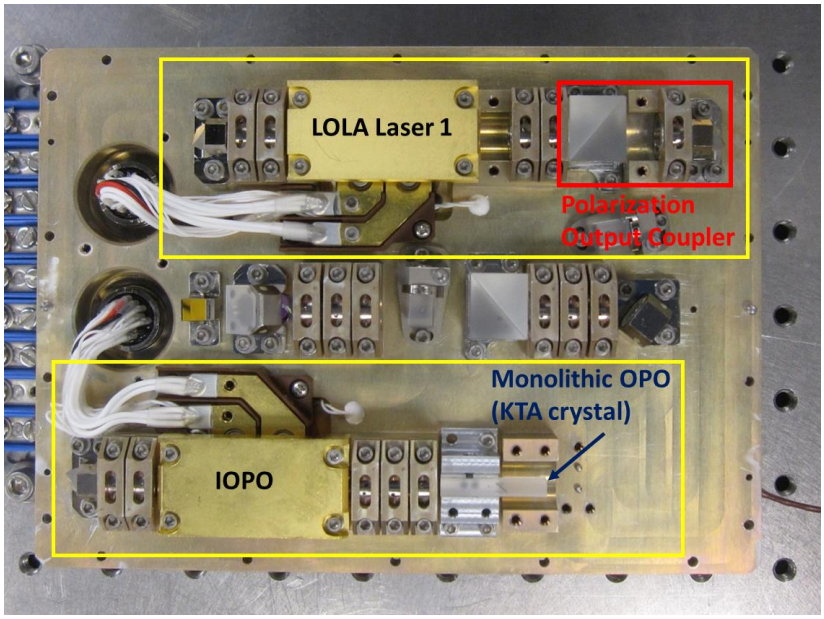

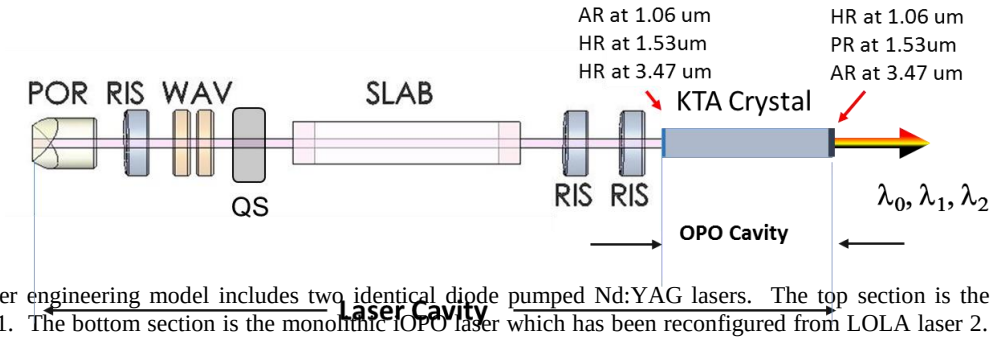

Figure 3. LOLA laser engineering model includes two identical diode pumped Nd:YAG lasers. The top section is the original LOLA laser 1. The bottom section is the monolithic iOPO laser which has been reconfigured from LOLA laser 2. The schematic shows the configuration of the iOPO. POR is Porro prism, RIS is Risley wedge, WAV is 0.57 waveplate, and QS is the passive Q-switch.

For 3.47 µm wavelength monolithic iOPO, a 4x4x24 mm^3 KTA crystal is used in non-critical phase matching (NCPM) to eliminate the walk-off effect with a maximum effective nonlinear coefficient. One end of the KTA crystal is coated for HT at the pump wavelength, 1064 nm, and HR at the signal wavelength, 1534 nm. The other end is HR coated at pump wavelength, partial reflection (R=80%) coated at the signal wavelength, and HT coated at the idler wavelength, 3480 nm. The crystal ends are parallel polished to less than 10 arcseconds to form a monolithic OPO cavity for signal wavelength at 1534 nm. The iOPO reaches threshold when the pump diodes current is ~70A and pump duration of 150 µs. The output energies at the idler and signal wavelengths are ~450 µJ and 1.2 mJ, respectively. Figure 5 shows the temporal profiles at the pump and signal wavelengths. We did not have a fast detector to measure the idler pulse width. Due to the OPO down conversion process, we expect the idler will have a similar pulse width as the signal. The 1534 nm signal pulse width is about 4 ns. The intracavity 1064 nm photons are rapidly converted to signal and idler photons when the iOPO reaches the threshold, which is clearly shown by the sharp trailing edge of the 1064 nm pulse in Figure 4 (a). The spectrum and spatial profile of the idler are shown in Figure 4 (b) and (c). To estimate the relative iOPO conversion efficiency, we replaced the iOPO monolithic crystal with a standard output coupler with R=50%. Under a similar pump condition, the 1064nm laser output is 3.1 mJ. The quantum conversion efficiency is 46%. We have made a copy of the iOPO laser for a mass spectrum instrument, which has been routinely operated for over six months.

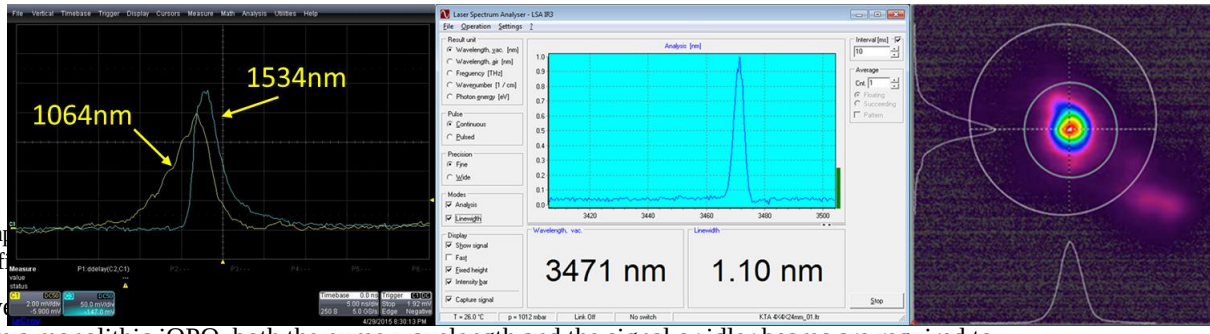

Figure 4. (a) The temp
The spatial beam prof

For 2.7 and 2.9 µm wave
(CPM). In order to form a monolithic iOPO, both the pump wavelength and the signal or idler beams are required to propagate collinearly. The two possible crystal cuts for KTP that meet this requirement are

For 2.7 µm generation:

Case (1) 2700 (o) + 1756 (e) = 1064 (o). Crystal cut for $\theta = 46.4^o$ and $\phi = 0^o$

Case (2) 2700 (e) + 1756 (o) = 1064 (o). Crystal cut for $\theta = 62.1^o$ and $\phi = 0^o$

For 2.9 µm generation:

Case (1) 2900 (o) + 1680 (e) = 1064 (o). Crystal cut for $\theta = 45.6^o$ and $\phi = 0^o$

Case (2) 2900 (e) + 1680 (o) = 1064 (o). Crystal cut for $\theta = 67.1^o$ and $\phi = 0^o$

where, o denotes the ordinary beam and e the extraordinary beam. We have developed a breadboard for initial experiments using case (1) crystals cut for 2.7 and 2.9 µm generation, shown in Figure 5. In this design, the pump and idler are both ordinary beams and propagate collinearly. The crystal ends are parallel polished to less than 10 arcseconds

to form a monolithic iOPO cavity for the idler wavelength. One crystal end is coated for HT at the pump wavelength and HR at the idler wavelength. The other end is coated for HR at the pump wavelength and PR (R=80%) at the idler wavelength.

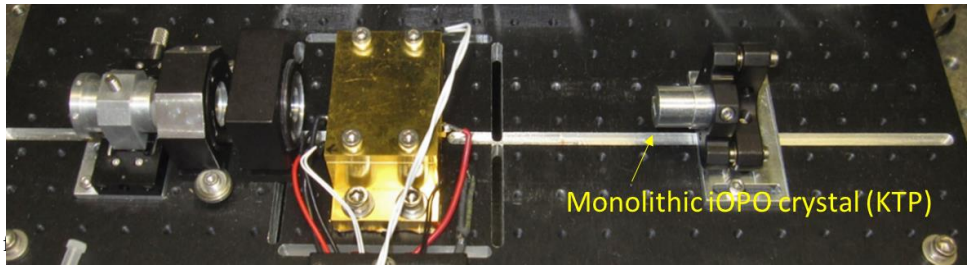

Figure 5. Breadboard i

The iOPO breadboard has the same optical design as the modified LOLA EM shown in Figure 3. We use a low Optical Density (OD) passive Q-switch for initial experiments to reduce the possibility of optical damage. We first tested the KTP crystal for 2700 nm iOPO. With the q-switch OD of 0.12, the iOPO reaches threshold when the pump diodes current is 32A and pump duration is 120 µs. The output energies at idler and signal wavelength are ~ 50 µJ and 150 µJ, respectively. Figure 6 shows the signal and idler spectrums measured with a Laser Spectrum Analyzer (HighFinesse, model LSA). The measured idler wavelength is 2652 nm, which is 48 nm shorter than the designed wavelength of 2700 nm. This is due to a fabrication error of the KTP crystal phase matching angle. The signal wavelength is 1778 nm.

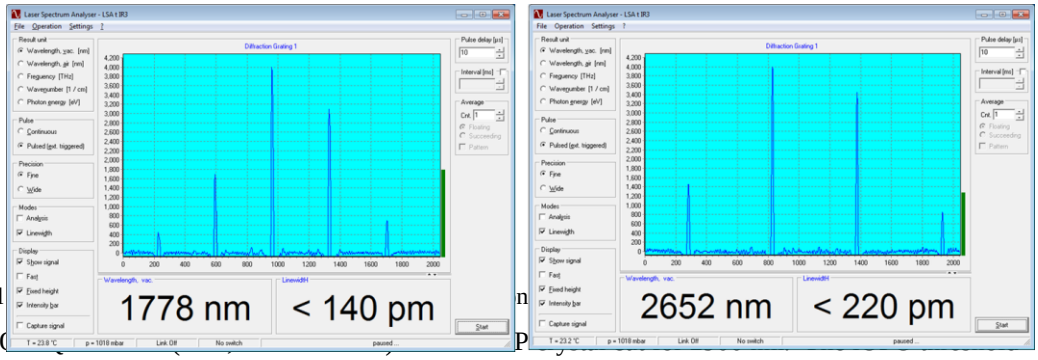

Figure 6. iOPO signal n

We have tested various O P
is much higher for 2900 nm than KTP for 2700 nm. The iOPO did not reach threshold with the 0.15 OD Q-switch in our initial attempt. With the 0.22 OD Q-switch, the 2900 nm iOPO lases for a few seconds before the KTP crystal surface damaged. Figure 7 shows the microscope image of the damaged optical coating of the KTP crystal. The damaged KTP surface is the one facing the Nd:YAG pump head. Both 2700 nm and 2900 nm KTP crystals were ordered from the same company at the same time. It is highly likely that the 2900 nm KTP crystal has a similar crystal cutting angle error as the 2700 nm. The actual KTP phase matching wavelength is likely to be 2852 nm instead of the specified 2900nm. We believe the high iOPO threshold is due to the high optical loss in the KTP crystal at the 2850 nm water absorption band. The vendor confirmed that their KTP crystal has ~5% absorption loss near 2850nm. The same water absorption issue is responsible for optical coatings damage. This is especially true for e-beam coating. We spent significant time discussing specifications with coating vendors for high performance optical coating at IR wavelengths. Unfortunately, the HR coating at 3 µm is very thick and usually has a lower damage threshold. We are also investigating the use of ion assisted deposition (IAD) and ion beam sputtering (IBS), which are less susceptible to moisture absorption and could improve the damage threshold of these coatings.

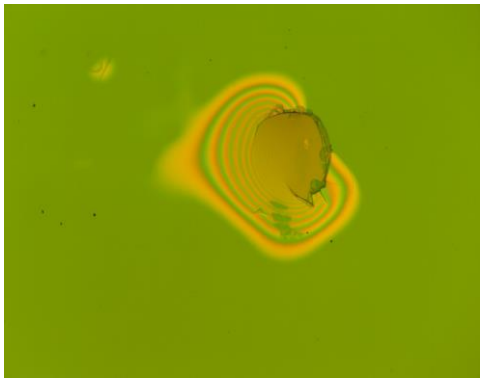

Figure 7. Microscope image of damaged optical coating on KTP crystals.

We have also designed and procured KTP crystals for generating 2700 nm and 2900 nm using case (2) crystal cut. The benefit of this design is that the optical coatings will be more robust and cheaper. In this design, pump and signal beams are ordinary beams and propagate collinearly in the crystal. The idler beam has a large walk off of about 35mrad, which could significantly degrade the idler's beam quality. We will use two 15 mm long KTP crystals oriented for walk-off compensated Type II critical phase matching to improve the idler beam quality and efficiency [12, 13]. The two crystals will be diffusion bonded, polished and coated to form a monolithic iOPO cavity. We are currently waiting for the crystal delivery.

To demonstrate efficient near-degenerate iOPO at 2.1 um for the potential Titan laser altimeter, we performed initial experiments using two existing KTP crystals in walk-off compensation configuration [12]. The KTP crystal size is 4x4x15 mm^3 and is cut at $\theta = 51.4^o$ and $\phi = 0^o$ for Type II CPM at 2128 nm. Both KTP end surfaces are AR coated at 2128 nm and 1064 nm. Figure 8 shows the experimental setup. M1 is a HR at 1064 nm. M2 is the iOPO mirror coated with R > 99.5% between 2000 – 2300 nm, T > 95% at 1064 nm for surface 1 and AR at 1064 nm for surface 2. M3 is the iOPO output coupler coated for PR = 60% between 2050-2200 nm and HR at 1064 nm for surface 1, AR between 2050-2200 nm for surface 2. With the Q-switch OD of 0.12, the iOPO reaches threshold when the pump diodes current is 33.9 A and pump duration is 120 us. The total output energy is 145 µJ per pulse. Figure 9 shows the near-degenerate iOPO output spectrum measured by Laser Spectrum Analyzer. We calibrated the LSA after we performed the experiment. The corrected wavelengths are 2109.5 nm and 2148.5 nm. To shift the wavelength to the Titan atmospheric transmission window between 1.99 to 2.08um, we plan to use diode pumped Yb:YAG crystal instead of Nd:YAG, which has a gain peak at 1.03 µm, as the iOPO pump source to generate 2.06 µm output.

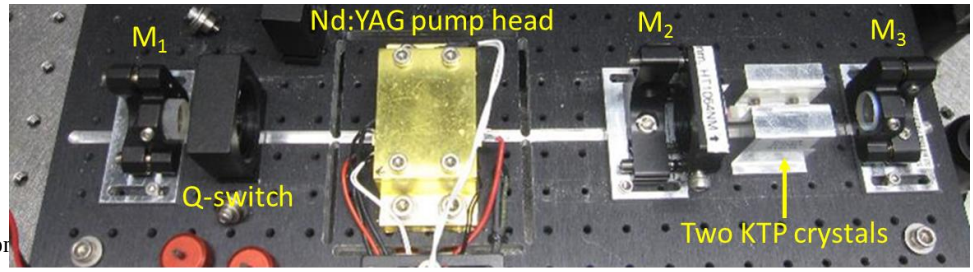

Figure 8. Walk-off cor

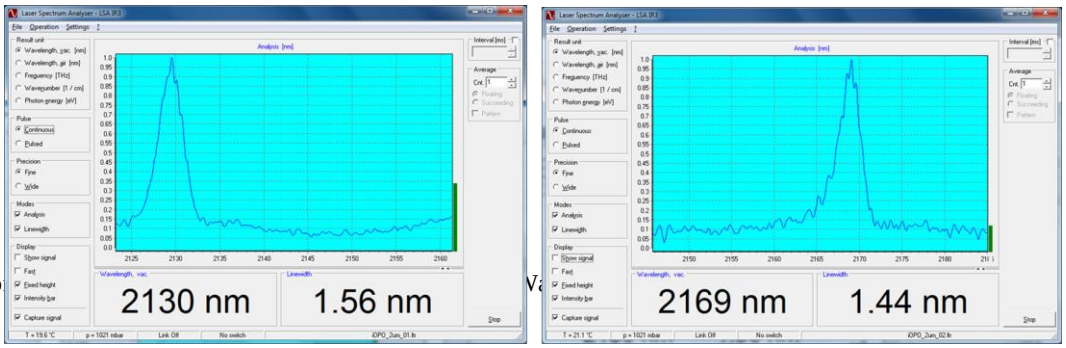

Figure 9. Walk-off co V
2148.5 nm.

3. CONCLUSIONS

We are currently developing laser transmitters for the NIR and MIR multi-wavelength lidar instruments. We have successfully demonstrated the new monolithic iOPO laser to generate desired wavelengths at 2.1 µm, 2.65 µm and 3.47 µm. Our monolithic iOPO transmitter design utilizes many years of space laser heritage and provides a direct path toward next generation spaceborne lidar and laser spectrometer at NIR and MIR wavelengths.

4. ACKNOWLEDGEMENTS

The authors acknowledge the support from the NASA GSFC's Internal Research and Development (IRAD).

REFERENCES

[1] Roger N. Clark, "Detection of Adsorbed Water and Hydroxyl on the Moon," Science 326(5952), 562-564 (2009), DOI:10.1126/science.1178105

[2] Deutsch, Ariel N., et al., "Comparison of areas in shadow from imaging and altimetry in the north polar region of Mercury and implications for polar ice deposits," Icarus, 280, 158-171 (2016), DOI:10.1016/j.icarus.2016.06.015

[3] Neumann G. A. et al., "Bright and dark polar deposits on Mercury: evidence for surface volatile," Science (2012), DOI:10.1126/science.1229764

[4] Zuber, M. T. et al., "Constraints on the volatile distribution within Shackleton crater at the lunar south pole," Nature, 486, 378–381 (2012), DOI:10.1038/nature11216

[5] Oshman, M. K., S. E. Harris, "Theory of optical parametric oscillation internal to the laser cavity," *IEEE J. Quantum Electron*. QE-4, 491–502 (1968), DOI:10.1109/JQE.1968.1075372

[6] T. Debuisschert, et al., "Intracavity optical parametric oscillator: study of the dynamics in pulsed regime," *J. Opt. Soc. Am. B*, 13, 1569-1586 (1996), DOI:10.1364/JOSAB.13.001569

[7] Wang, Y. et al., "Passively Q-switched quasi-continuous-wave diode-pumped intracavity optical parametric oscillator at 1.57 µm", *China Phys Lett,* 25, 4009-4012 (2008)

[8] Fahey, M. E. et al., "Advanced laser architecture for the two-step laser tandem mass spectrometer," *Proc. SPIE* 9834, *Laser Technology for Defense and Security XII*, 983409, DOI:10.1117/12.2227141

[9] Anthony W. Yu, et al., "The Lunar Orbiter Laser Altimeter (LOLA) laser transmitter," International Geoscience and Remote Sensing Symposium (IGARSS), 3378-3379 (2011), DOI: 10.1109/IGARSS.2011.6049943

[10] Yu, AW, Shaw, GB, Novo-Gradac AM, Li SX, Cavanaugh J., "In Space performance of the Lunar Orbiter Laser Altimeter (LOLA) laser transmitter," Proc. SPIE 8182, 818208 (2011), DOI: 10.1117/12.898546

[11] Private conversation.

[12] R. F. Wu, et al., "Compact 21-W 2-µm intracavity optical parametric oscillator," Opt. Lett. 25, 1460-1462 (2000), DOI:10.1364/OL.25.001460

[13] Xiaodong Mu, et al., "Optical parametric oscillations of 2 µm in multiple-layer bonded walk-off compensated KTP stacks", Opt. Lett. 35, 387-389 (2010), DOI: 10.1364/OL.35.000387